Engineering Science and Technology, an International Journal 54 (2024) 101726

Contents lists available at ScienceDirect

Engineering Science and Technology, an International Journal

journal homepage: www.elsevier.com/locate/jestch

Full Length Article

Influence of the cutting-edge preparation in ceramic tools for grooving of Inconel® 718 and force prediction

Pablo Fernández-Lucio [a,b,*], Gorka Urbikain [a,b], Soraya Plaza [a,b], Octavio Pereira [b]

[a] Department of Mechanical Engineering, University of the Basque Country (UPV/EHU), Plaza Torres de Quevedo S/n, Bilbao 48013, Spain
[b] Aeronautics Advanced Manufacturing Centre (CFAA), University of the Basque Country (UPV/EHU), Zamudio 48170, Spain

ARTICLE INFO

Keywords:
Inconel® 718
Whisker reinforced alumina
Cutting edge preparation
Turning
Orthogonal cutting

ABSTRACT

The machining of slots in aeronautical turbine cases and discs is an extremely delicate operation. First, these parts require materials with excellent wear, high temperature and corrosion properties, such as the low machinability materials of the S group. Secondly, as this is one of the last turning operations, the value of the part is already considerable and any machining error can be dramatic. Traditionally, carbide tools have been the choice due to their greater safety and precision control. However, ceramic inserts offer unquestionable advantages in terms of higher cutting speeds and lower cost per part. Nonetheless, the behaviour of these cutting tools has a much narrower application interval (i.e. optimal set of cutting parameters) than carbide inserts. Machine workers need reliability. This work analyses the performance of ceramics, specifically, whiskers reinforced alumina type ceramics in the machining of grooves on Inconel® 718. Specifically, it analyses the effects of edge rounding, wear and other cutting parameters on cutting forces, and proposes a predictive model for grooving including the above parameters (rounding, wear and feed) for the first time. The validation results gave relative errors of 1.5% in the tangential component, and 4.8% in the feed component. As a result, it can be stated that the rounding radius affects more feed components than tangential ones, being, moreover, more critical to wear. Furthermore, smaller feeds and bigger cutting edge radii delay the apparition of flank wear.

1. Introduction

Turbomachinery components, such as cases or disks, require materials that withstand extreme working conditions. Inconel® 718 is one of those nickel-based alloys that maintains its excellent mechanical and physical properties at high temperatures making it a feasible material to use in those components [1]. However, when machining its thermo-mechanical properties pose big issues, making it a low machinability material: low material removal rates, extreme tool wear and very high cutting forces [2]. Researchers, like Ulutan and Ozel [3] and Del Sol et al. [4], affirm that those materials' properties and the high requirements for the final parts make machining operations in those components a complex challenge.

Traditionally, for the machining of these kinds of components cemented carbide tools are used because of greater safety and precision control. Nonetheless, due to the fact that cemented carbide is considered a raw material [5] and to the aim of enhancing productivity, ceramic tools are presented as a solution to it by achieving high cutting speeds thanks to their good abrasion resistance [6] and hardness [7]. Alumina tools with reinforcements, like TiC, TiCN or whiskers of SiC, effectively improve the thermal shock resistance [8] and fracture toughness of alumina matrix [9], which is brittle and with low tensile strength, becoming feasible materials to substitute cemented carbide tools in the machining of difficult-to-cut materials [10]. In fact, owing to the fact that turning operations are very stable and continuous, ceramic tools present a higher material removal ratio and tool life than cemented carbide ones [11].

In turbine cases and disks, turning represents about 45 % and 60 % respectively of total machining operations. These components have big diameters which entails the use of great lathe-milling vertical centres. However, some of the operations, such as the machining of the grooves in aeronautical turbine cases, are an extremely delicate operation (see Fig. 1). Therefore, any improvement in machining times or tool's life is of great value for manufacturers. Despite the complexity of machining, there is a trend towards high-performance machining in the aeronautical industry.

The machining of the slots is one of the last turning operations, the value of the part is already considerable and any machining error can be

* Corresponding author.
E-mail address: pablo.fernandezd@ehu.eus (P. Fernández-Lucio).

https://doi.org/10.1016/j.jestch.2024.101726
Received 29 February 2024; Received in revised form 17 May 2024; Accepted 24 May 2024
Available online 28 May 2024

Fig. 1. Aeronautical turbine case and a cutting section view.

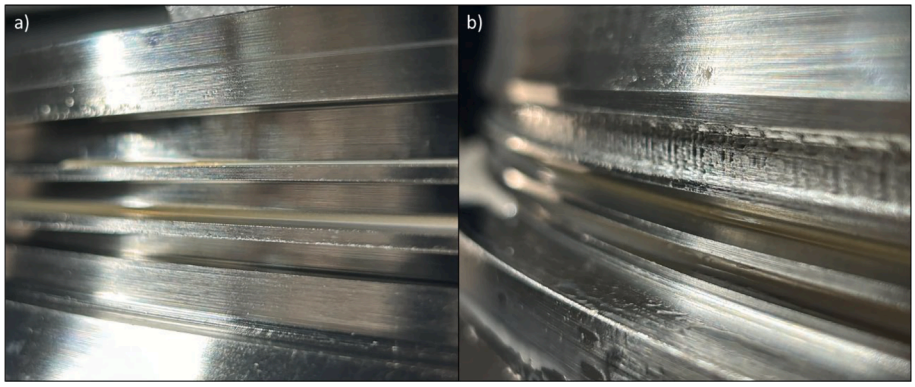

Fig. 2. Good cutting edge preparation that led to optimal finishing (a) and excessive rounding that led to tool breakage (b) in the machining of Inconel® 718.

Table 1
SiC whiskers reinforced alumina properties.

Density	Hardness	Transverse Rupture Strength	Thermal Expansion	Thermal Conductivity
3.74 $g{\cdot}cm^{-3}$	2100 HV	690 MPa	$6{\cdot}10^{-6}\ {}^{\circ}C^{-1}$	35 $W{\cdot}(m{\cdot}K)^{-1}$

dramatic. A tool with a rounded cutting edge means that the material to be machined is pushed into the chip and onto the machined surface. The material pushed by the effect of the rounded cutting edge is called the Dead Metal Zone (DMZ). Researchers, such as Agmell et al. [12] and Hu et al. [13], define the DMZ as the zone in which the chip appears to be stagnant, but, since it does not have zero velocity, it follows that there is a separation within the DMZ.

The size of the cutting edge radius has a great influence on the ploughing effect as the larger the radius, the larger the resulting DMZ area and thus the ploughing effect affecting the cutting process. Nonetheless, including a rounded edge helps to strengthen the cutting edge, making it more resistant to thermos-mechanical loads [14]. This behaviour is corroborated by Bouzakis et al. [15], Zhao et al. [16], Vopat et al. [17], and Hariprasad et al. [18], where they achieved longer tool's life by rounding cutting edges (Fig. 2a). Even so, they also concluded that, if the rounding is excessive, it is harmful to the tool's life that could break affecting the workpiece (Fig. 2b). That is why in those operations the correct preparation of the tool's cutting edge is key for optimal machining: a sharp edge is very fragile to machine difficult-to-cut materials, while an excessively blunt edge is detrimental to the cutting force. This is even more relevant when machining with ceramic tools because of its brittleness.

To see the effect of cutting edge preparation on the cutting forces during machining, some authors have modelled it from different approaches. In their study, Sela et al. [19] developed a regression model to predict cutting forces in an alloy of aeronautical aluminium with the tool's cutting edge radius and the feed used in broaching. After

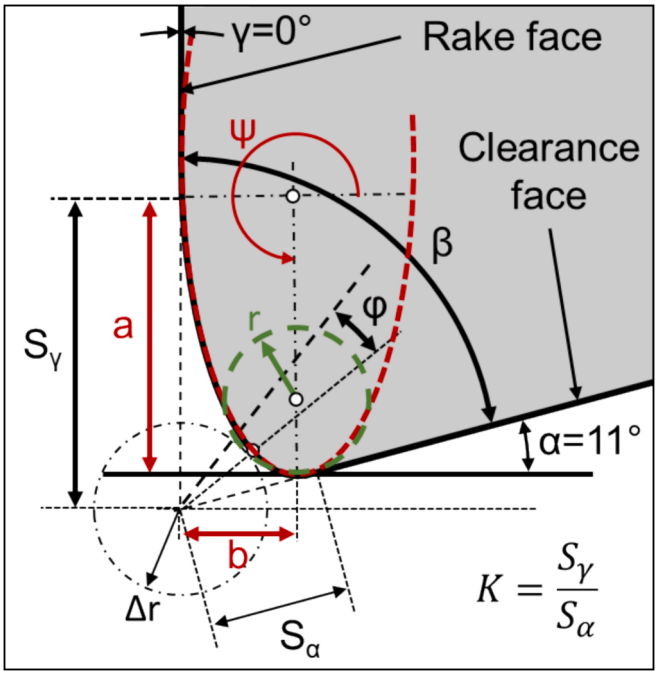

Fig. 3. Profile values obtained with Alicona® Infinite Focus G5 software.

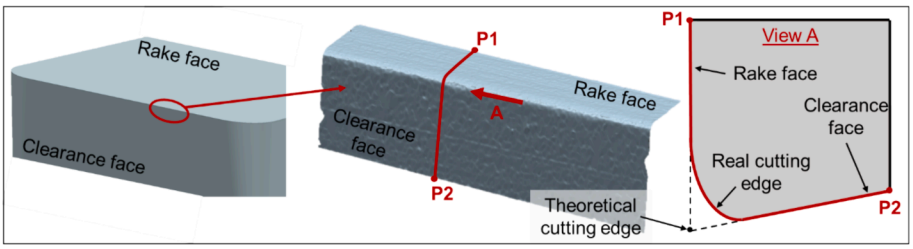

Fig. 4. Alicona® Infinite Focus G5 software method to obtain an average profile.

Table 2
Cutting edge parameters for tested tools.

Tool	Parameters proposed in Denkena [22]				Equivalent radius
	S_α [μm]	S_γ [μm]	Δr [μm]	φ [°]	r_{eq} [μm]
01	16	19	8	−1.7	14
02	17	22	9	−3.3	16
03	23	28	12	−3.1	20
04	32	35	16	−1.1	27
05	18	23	9	−3.2	16
06	24	25	11	−0.3	20
07	29	32	14	−1.5	24
08	18	23	10	−3.2	16
09	24	25	12	−1.0	20

Table 3
Chemical composition and mechanical properties of tested Inconel® 718.

Chemical composition [%]								
Cr	Fe	Nb	Mo	Ti	Si	C	Other	Ni
19.30	17.20	5.21	3.05	1.00	0.06	0.03	0.95	Balance
Mechanical Properties								
Hardness	Young's Modulus	Tensile strength	Specific heat	Melting temperature	Thermal conductivity			
45 HRC	206 GPa	1730 MPa	461 J·(kg·K)$^{-1}$	1600 K	15 W·(m·°C)$^{-1}$			

obtaining the coefficients, they did another test to validate the model, achieving relative errors of less than 3 %. In another study, Uysal and Altan [20] analysed the influence of cutting edge radius in the machining of copper by modelling the cutting forces and the effect of the radius on the ploughing force using a slip-line field model. With it, authors concluded that, as the radius of the cutting edge increases, the ploughing and thrust effect that was generated increases. Jagadesh and Samuel [21] compared forces generated during machining of Ti6Al4V with the predicted ones by a FEM model and by a mechanistic model. After doing comparisons, they concluded that the mechanistic model was more precise than the FEM one. The relative errors were 9.7 % for the mechanistic predictions and 11.4 % for FEM predictions.

In view of the above, it has been found that there are no cutting models in the literature that predict the forces with a ceramic tool for machining Inconel® 718 taking into account cutting edge radius. Therefore, considering the importance during machining of difficult-to-cut materials of the cutting edge preparation, the novelty of the work here presented is to machine grooves in Inconel® 718 using whiskers reinforced alumina tools with different cutting edge preparation to analyse its behaviour. For this purpose, section 2 defines the basic parameters in tool geometry affecting metal cutting and chip creation. In section 3 the experimental procedure to carry on the tests is explained. Section 4 presents and discusses tool wear, chip morphology and cutting forces. Furthermore, in section 5 a mechanistic model, which takes into account tool wear and cutting edge radius, has been proposed with the aim of predicting cutting forces during the machining of this kind of critical operation. Finally, section 6 resumes all the conclusions and discussions made over the discussion.

Table 4
Cutting parameters for each tested tool.

Tool	r_{eq} [μm]	v_c [μm]	a_p [μm]	f [μm]
01	14	300	3.18	0.05
02	16	300	3.18	0.05
03	20	300	3.18	0.05
04	27	300	3.18	0.05
05	16	300	3.18	0.07
06	20	300	3.18	0.07
07	24	300	3.18	0.07
08	16	300	3.18	0.10
09	20	300	3.18	0.10

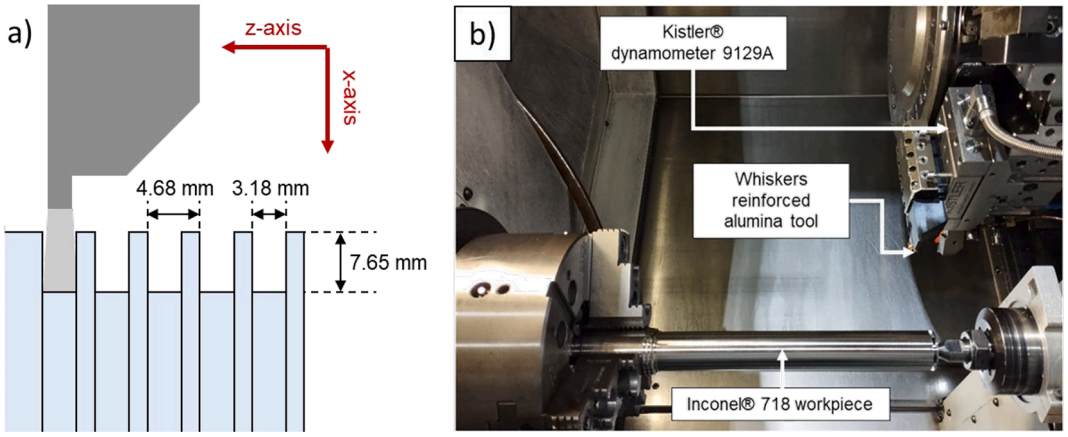

Fig. 5. a) Grooves manufacturing scheme; b) experimental setup.

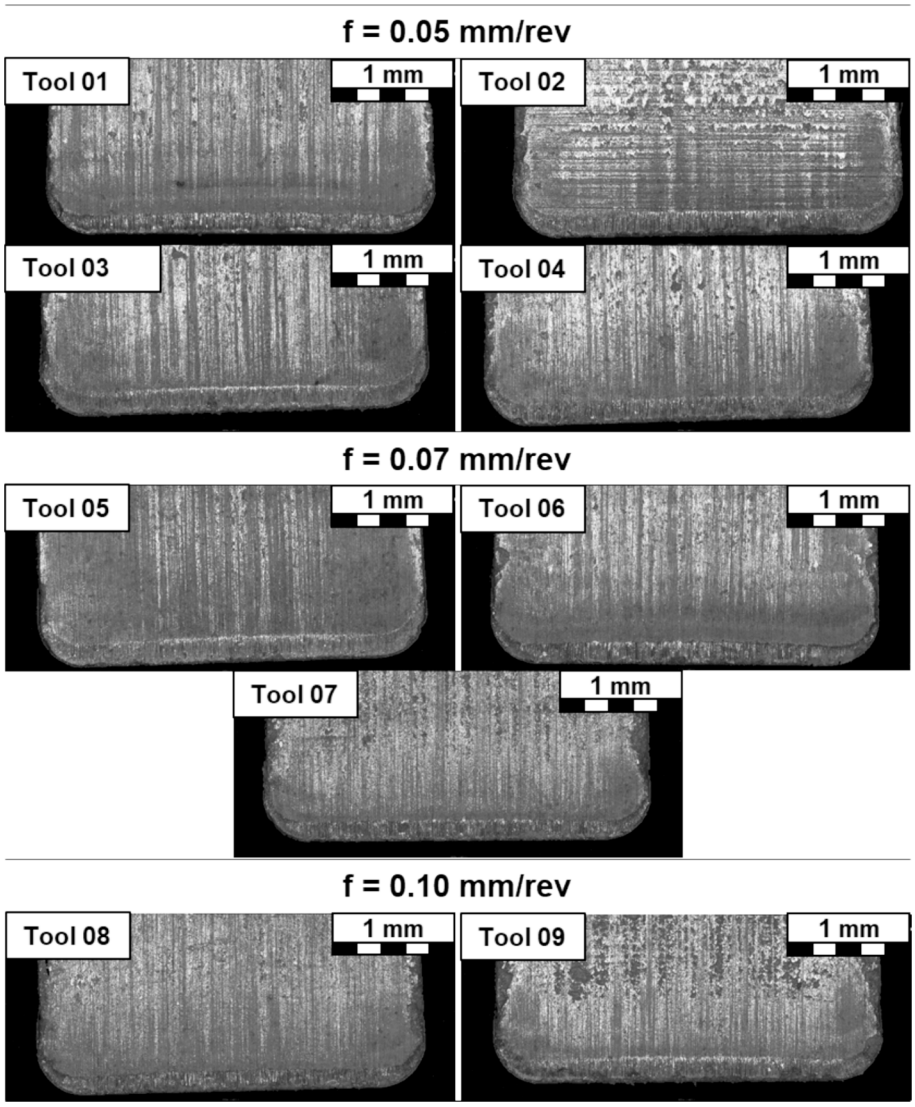

Fig. 6. Rake face of each tool after the cutting tests.

2. Definition of tool geometry

The first thing done to carry out this study was the measurement of the edges of the cutting tools. Tools were provided by Greenleaf Corporation® and the geometry was WG-4125-1A type made up of SiC whiskers reinforced alumina with 28 % SiC called WG-300. Its main properties are shown in Table 1. These tools have a rake angle of 0° and a clearance angle of 11° (see Fig. 3) left by the tool holder whose ISO designation was 415316-125VGS from the same manufacturer as the inserts. This manufacturer offers a great variability of cutting edge radii between 10 and 30 μm. To measure the cutting edges an Alicona® Infinite Focus G5 microscope has been used which defines the cutting edge with Denkena parameters. However, the software also approximates the edge to a circle as can be seen in Fig. 3.

The microscope scans the cutting edge and, from the 3D model generated, the software performs a series of slices (50 in this study) obtaining a series of profiles (see Fig. 4). These profiles are used to produce an average profile in which all the Denkena parameters [22] are measured and the equivalent radius is calculated. For the equivalent radius, the software uses a minimum square approximation and is the parameter used for the cutting forces predictive model presented in section 5. The equivalent radius is a parameter that defines in a simple way the geometry of the cutting edge between the clearance and rake faces. Table 2 shows all cutting edge parameters of tested tools. A total of 9 cutting edges were used for the tests and each tool was measured three times.

3. Experimental setup

This section presents the experimental procedure carried out during the grooving tests on aged Inconel® 718. Table 3 shows the chemical composition and mechanical properties of the alloy.

Fig. 5a shows the followed procedure for the preparation of slots. The initial diameter of the workpiece was 42 mm and the depth of the groove was 7.65 mm due to geometry limitations of the tool holder. Between each groove, a 1.5 mm separation was established to avoid dynamic problems and vibrations and to ensure rigid cutting. Under this approach, due to the characteristics of the tool, the tool holder and the process itself, these tests can be considered as orthogonal cutting.

All the tests were carried out in a CMZ TC25BTY turning centre with 35 kW of spindle power and integral spindle. Cutting forces were registered with a triaxial Kistler® 9192A piezoelectric dynamometer and an OROS® OR35 real-time multi-analyser with a sample frequency of 12,800 samples/s (see Fig. 5b). Moreover, after machining each groove a picture of the tool was taken with a PCE-200® microscope to analyse wear. The end of the test criteria was to make five grooves,

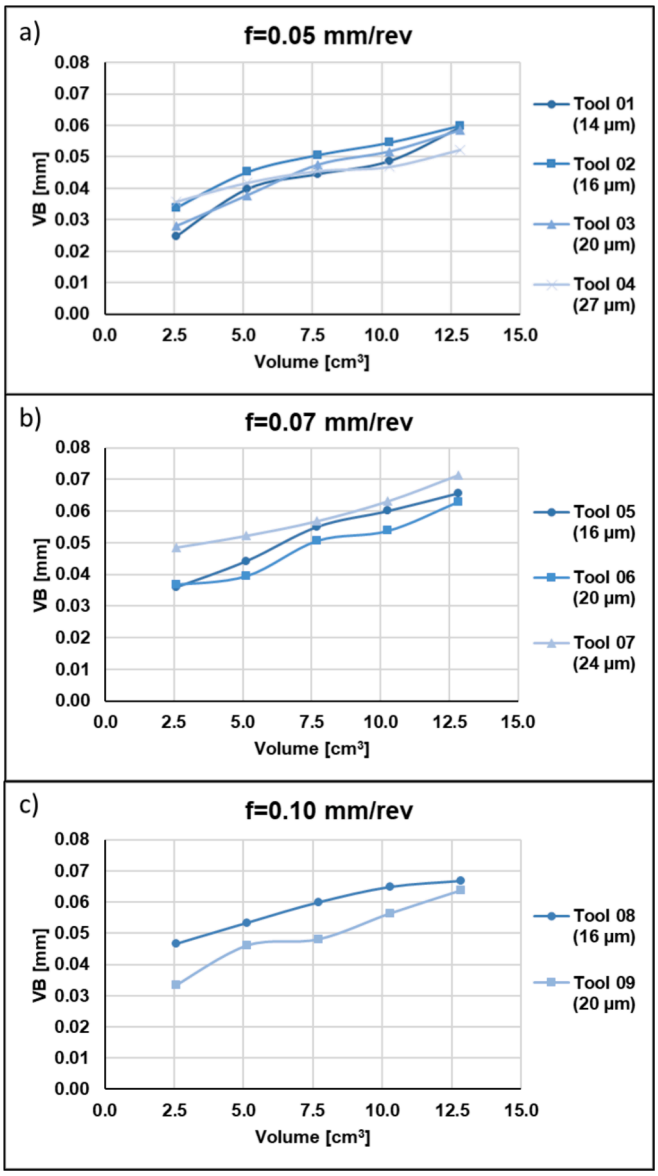

Fig. 7. Flank wear against removed chip volume with a feed of 0.05 mm/rev (a), 0.07 mm/rev (b) and 0.10 mm/rev (c).

obtain a flank wear of 0.12 mm or premature breakage of the insert. This flank wear limit was chosen because the tolerances of the slots in components in the aeronautical sector are very tight and, having a 0.12 mm flank wear with this tool implies a loss of edge of 23 µm, which would leave the slot outside these tolerances. Chip was also collected after the first groove of each tool with the aim of verifying chip-tool contact interactions.

Cutting parameters for the tests were a cutting speed of 300 m/min and three different feeds: 0.05, 0.07 and 0.10 mm/rev. The depth of cut was kept constant and equal to the grooving insert width of 3.18 mm. These cutting parameters were set in accordance with the tool manufacturer's recommendations. On the one hand, in the case of cutting speed, tests have been carried out with the maximum of the range proposed by the manufacturer (180–300 m/min). Nevertheless, it was noticed that using low speeds could result in tool breakage. When using a lower cutting speed, the temperature reached by the material is lower and the size of the DMZ is greater increasing cutting forces [23]; as there is no softening on the material, the tool breaks. For this reason, the cutting speed has been set at 300 m/min in the tests. On the other hand, the tool manufacturer recommends using a feed rate between 0.05 and 0.10 mm/rev. Therefore, in order to test the performance of the different cutting edge preparations under different conditions, it has been decided to use the three feeds indicated above the minimum of the range, the maximum and an intermediate one that is not halfway between the other two. Furthermore, during the tests, a synthetic oil solution of 10 % was injected at 6 bars as recommended by the manufacturer. Table 4 shows the cutting conditions for each of the tools tested.

4. Results and discussion

First, tool wear measurements in both rake and clearance faces are presented and discussed. Hereafter, chip morphology will be analysed. Finally, the cutting forces generated during machining are commented.

4.1. Tool wear

This section presents the measurement results of tool wear in both rake and clearance faces. To do so, feed influence on the chip-tool contact length and flank wear against chip-evacuated volume will be studied. All tested tools could make the expected five slots. Fig. 6 shows the rake face of each tool after ending all cutting tests. It can be seen clearly chip flow marks on the rake face and the crater left by the chip on the tools. None of the tools suffered excessive crater wear. Nevertheless, due to the tool exit of the slot, it can be observed a small chipping at the tool side. That chipping is not harmful to the tools and, thus, it is not a problem for machining unless excessive. However, the chipping level is acceptable within this margin.

Fig. 7 shows the flank wear for all tested tools. As can be seen, there is a great correlation between flank wear and removed chip volume. However, the relation among feed of used radii is not as clear. To clarify it, the correlation coefficient for each parameter (feed and equivalent radius) and the interaction of feed and equivalent radius with flank wear have been calculated. The correlation coefficient of two variables indicates its linear dependency and, in this case, specifies that there is no correlation between wear and cutting edge radii. Nevertheless, there is a weak linear dependence concerning the used feed and the interaction of feed and cutting edge radii with flank wear. According to that weak dependence, an increment in feed implies an increase in the tool's flank wear. With the cutting edge radii, the opposite is true: bigger radii reduce flank wear. Nonetheless, as the dependence is weak, chip evacuated volume is more dominant.

4.2. Chip morphology

Fig. 8 shows the obtained chip after the first machined slot of each tested tool. According to the classification of chip morphology of the standard ISO 3685:1993, all tools have generated a tubular and long chip shape, except for tool 06, which has been tubular and snarled. Those morphologies are typical in this type of operation. In grooving, breaking the chip is very complicated, and therefore, long chips are generated with the risk of becoming entangled in the tool, potentially leading to breakage. It must be highlighted that chips generated with a feed rate of 0.10 mm/rev had a much higher temperature than the others, making their collection difficult without using gloves.

As chip morphology is related to the way it flows through the rake face of the tool, it is possible to understand its behaviour during the cutting process. In this case, chips have moved away from the workpiece and in the opposite direction to the feed, which has helped to evacuate them without damaging the machined surface or being entangled in the tool. Additionally, it should be noticed that the diameters of the chips with feeds of 0.07 and 0.10 mm/rev (tools 05, 06, 07, 08, and 09) are larger than those generated with a feed of 0.05 mm/rev. This smaller diameter implies that the force generated at the contact between the chip and the rake face imparts a greater curvature to the chip. This is explained due to the smaller chip thickness generated under the feed of 0.05 mm/rev compared to the other two. A large curvature makes the

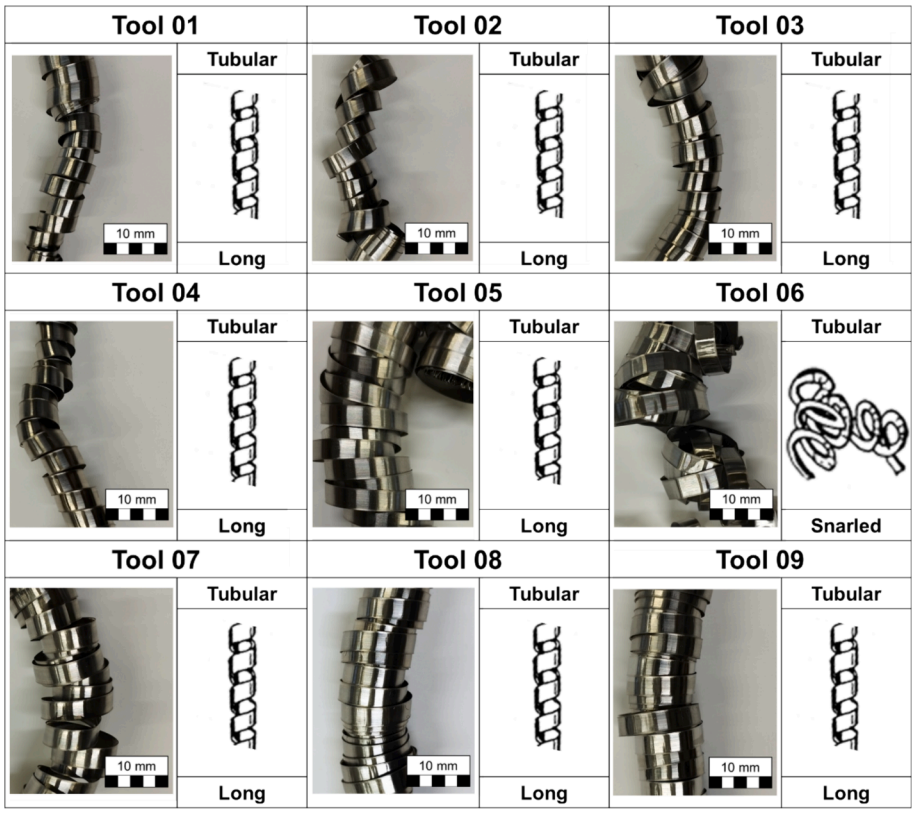

Fig. 8. Morphology and classification of obtained chip in the first groove for each tool according to ISO 3685: 1993 [25].

chip and the rake face separate earlier, which reduces contact length and, thus, wear of the rake face [24].

Fig. 9 shows SEM images of the obtained chip in the first groove of each tool viewed from the surface in contact with the tool's rake face. All images have something in common: feed marks can be seen. These marks are very typical in any turning process due to the friction between the chip and the tool's rake face.

Moreover, some of the generated chips (tools 01, 03, 04, 07, and 09) presented small and sporadic zones of oxidation. The absence of oxidation implies that the process was very thermally stable, thanks to effective lubrication-cooling in the cutting zone. Therefore, this fact can be considered negligible for all the cases analysed.

Finally, it should be specified that tools with bigger cutting edge radii (tools 03, 04, 08, and 09) appeared with drag marks some of them barely imperceptible (tool 09). Those marks are due to the ploughing zone in which the material of the dead metal zone is dragged along the cutting edge. In some cases that material could be attached to the cutting edge causing a huge increase in the cutting forces when pulling it out. Therefore, as this effect is only perceptible with big a cutting edge radius, it can be considered that chips flowed along the tool's rake face with no impediment.

4.3. Cutting forces

Fig. 10a shows the cutting forces generated during the machining of a slot. As can be seen in the figure, binormal force (F_b) is not relevant compared with the other two force components. Hence, it will be neglected through this study: the assumption of pure orthogonal cutting is valid. Secondly, from each machined groove, it has been obtained the initial and final values of the cutting forces. As there are no peaks at the entrance or exit of the cutting tool, forces can be easily tracked from subsequent passes (see Fig. 10b). The initial values are practically the same as the final ones of the previous groove. In this way, and as this principle of continuity is fulfilled, the cutting forces can be known at any instant of machining regardless of which slot the tool is machining.

Fig. 11 depicts the tangential forces (F_c) for all tested tools. This force component seems not to be affected by the different cutting edge radii. As can be seen, all the forces (from the 9 tools) can be grouped in three lines corresponding with the three feeds used for the machining tests. It is also noted that tool 6 generated a minor tangential force during the machining of the first groove. This behaviour was due to a modification of the feed used during the first slot to see the influence of changing feed in the middle of its lifespan. However, after the second slot tangential force for that tool regrouped with the tools that used a feed of 0.07 mm/rev. Overall, the slope for all curves is positive, something logical as wear increases, but they were very small. These may be due to the fact of using inserts with 0° rake angle and so, wear is not greatly affected in this force component, but in the feed direction.

Different behaviour was seen with feed components (F_f) of the generated forces. Fig. 12 is separated into three according to the feed used to carry out machining tests: Fig. 12a shows tools with 0.05 mm/rev; Fig. 12b with 0.07 mm/rev; and Fig. 12c with 0.10 mm/rev. The first thing that can be seen is that the difference in using different cutting edge radii is noticeable, especially when machining the first groove. In fact, using a radius of 14 μm cutting edge in the machining of the first slot with a feed of 0.05 mm/rev can reduce feed force by 30 % compared to using a radius of 27 μm. This is in accordance with the studies of Uysal and Altan [26], Wyen and Wegener [27], Li and Chang [28], and Liu et al. [29] among others, in which they concluded that the ploughing effect has more influence on feed components than on tangential.

To prove the existence of the ploughing effect during the machining of slots with SiC whiskers reinforced alumina tools, a quick-stop test has been done to see the DMZ and how the chip flows in that zone. For this test, a tool with 16 μm of equivalent cutting edge radius was used with a feed of 0.05 mm/rev and a cutting speed of 300 m/min. In Fig. 13 the chip formation instant is presented, where the DMZ can be seen and the two flows of the material: one in the chip flow direction and the other one under the cutting tool radius.

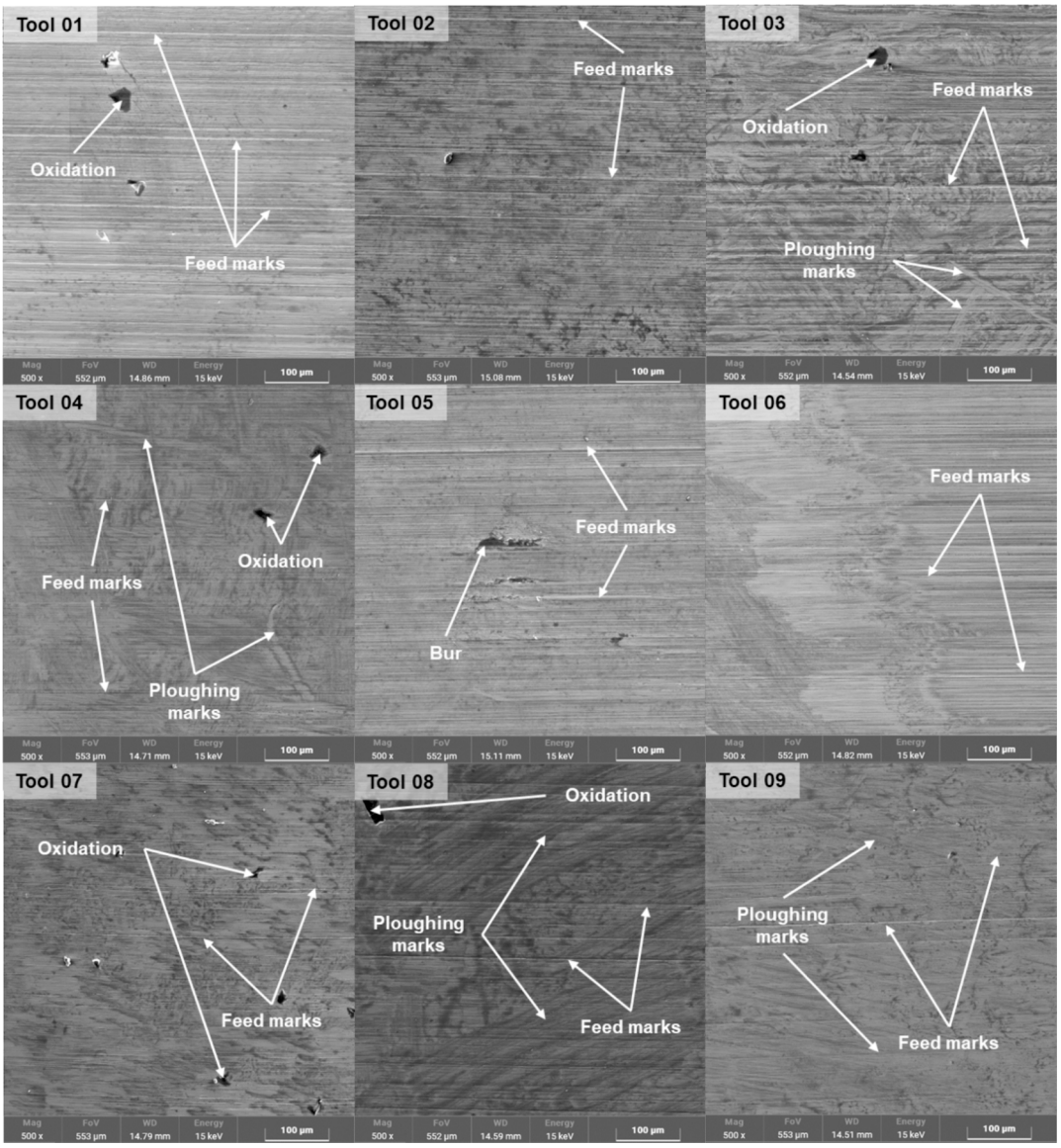

Fig. 9. SEM images of the chip on the machined surface for each tool.

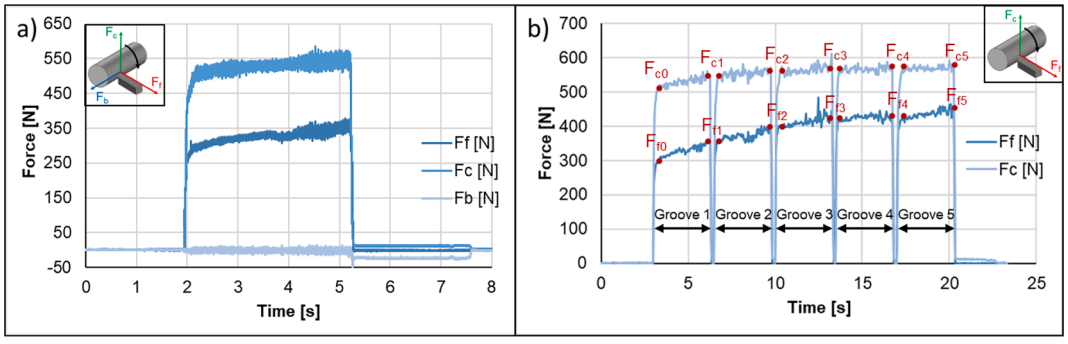

Fig. 10. a) Feed, tangential and binormal forces generated during the machining of a slot; b) tangential and feed force during one of the tests made.

Another thing that can be seen is that in this component, the influence of wear is noticeable from one groove to the next. This influence of wear also means that the initial differences by machining with different radii tend to become narrower. In view of the slope, it is very likely that the influence of the cutting edge radius will disappear in the subsequent grooves to be machined, with wear being the predominant factor. This is due to the gradual disappearance of the rounding of the cutting edge as the tool wear increases, as depicted in Fig. 14 for tool 02 and tool 04.

Furthermore, it can be seen how the effect of the radius had less influence on the feed force as the tool feed rate increased since, as can be seen in Fig. 12c with a feed rate of 0.10 mm/rev, there is hardly any difference between using one radius or the other. This can be explained

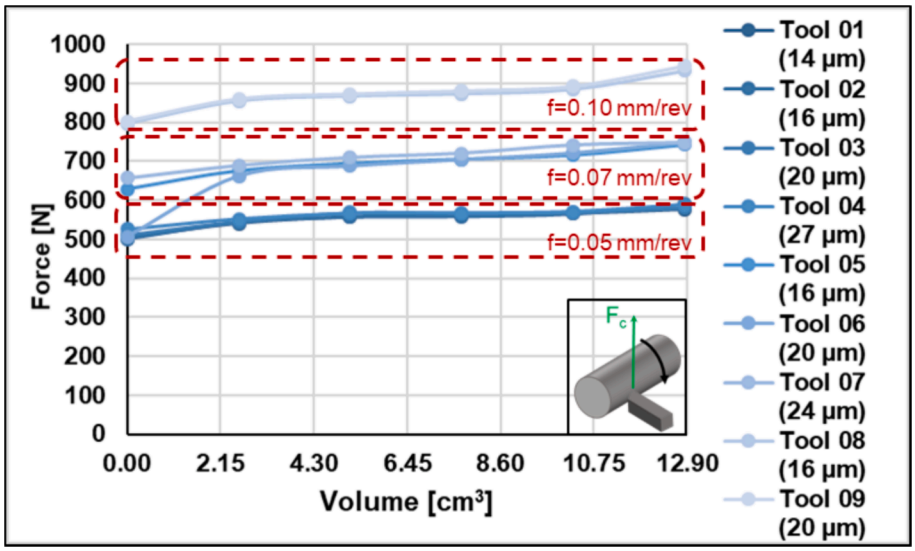

Fig. 11. Tangential force (F_c) for all tested tools.

by the fact that the effect of the ploughing force becomes less important at higher feed rates.

5. Cutting force model including wear and tool preparation

In view of the direct relationship between cutting edge radii and machining parameters with the generated forces during the cutting of Inconel® 718 with whiskers reinforced alumina tools in grooving operations, it was decided to model the tangential and feed cutting forces from the geometrical data of the tools and the machining parameters to be used. To analyse the performance of the proposed force model, it has been compared with a traditional and commonly used mechanistic cutting force model. Thus, the improvements of the proposed model can be quantified.

Table 5 shows the data used to obtain the coefficients for the traditional and the proposed model. Three different levels of wear were used for each of the selected tools (also three) that had three different radii. As the cutting speed has been equal for all the tests, it will be neglected in the obtaining of the coefficients.

5.1. A mechanistic cutting force model

The mechanistic model commonly used and cited in the literature is the one proposed by Budak et al. [30] and, hence, is the one selected to make the comparison. Equation (1) and Equation (2) show that proposal with the addition of a wear component.

$$F_{ct} = k_{sct} \cdot f + k_{fct} + k_{wct} \cdot VB \tag{1}$$

$$F_{ft} = k_{sft} \cdot f + k_{fft} + k_{wft} \cdot VB \tag{2}$$

Table 6 shows the obtained six coefficients for the proposed mechanistic cutting force model.

Viewing those coefficients it should be noticed that, as it was expected, the weight of flank wear in forces generation is greater in the feed component than in the tangential component ($k_{wft} > k_{wct}$). Another important thing is that friction also has more influence on the feed force component.

5.2. Proposing a new cutting force model

As the commonly used model proposed by Budak, Altintas and Armarego, the generation of the cutting forces in this model is also divided into two components apart from the wear component; shear and friction. The novelty resides in two factors. On the one hand, it has been included as a correcting factor to the friction component as a function of the cutting edge radii and the used feed. This has been done because it has been assumed that, as the ratio between the radii and the feed increases, the most affected component should be the friction component as the ploughing increases and, therefore, the friction of the chip with the tool as it slides along the cutting surface.

On the other hand, to include the effect of feed on the cutting temperature that softens the machined material, a correction of the k_{sct} and k_{sft} has been added. To do that, it has been proposed to include a new coefficient that depends on a reference feed and the used one. In this case, the reference feed has been established in 0.05 mm/rev. Those two modifications can be seen in Equation (3) and Equation (4).

$$F_{cm} = \left(k_{scm1} - k_{scm2} \cdot \frac{f - f_{ref}}{f_{ref}}\right) \cdot f + k_{fcm} \cdot \frac{r_{eq}}{f} + k_{wcm} \cdot VB \tag{3}$$

$$F_{fm} = \left(k_{sfm1} - k_{sfm2} \cdot \frac{f - f_{ref}}{f_{ref}}\right) \cdot f + k_{ffm} \cdot \frac{r_{eq}}{f} + k_{wfm} \cdot VB \tag{4}$$

Table 7 shows the eight obtained coefficients for the proposed mechanistic cutting force model.

As in the traditional model, the feed component is more affected by wear than the tangential component. Similar behaviour happens with the friction in which feed cutting force component is more susceptible to cutting edge radii. Furthermore, compared to the traditional mechanistic model, the weight of wear is almost the same while the friction has decreased for the tangential component.

6. Model validation

After obtaining the coefficients for both mechanistic force models, the validation of each one has been done with all the measured forces and wear. Fig. 15 shows the comparison between the real forces and the predicted forces and the error for both predictions and both components for all tested tools. Notice that the data used for obtaining the coefficients are not shown in the figure. F_{cr} and F_{fr} are the real forces measured with the dynamometer for the tangential and the feed force, respectively. F_{ct} and F_{ft} are the predicted forces with the commonly used mechanistic model. F_{cm} and F_{fm} are the predicted forces with the proposed mechanistic model.

It can be seen that errors were reduced by applying the proposed model compared with the traditional one for both components of the

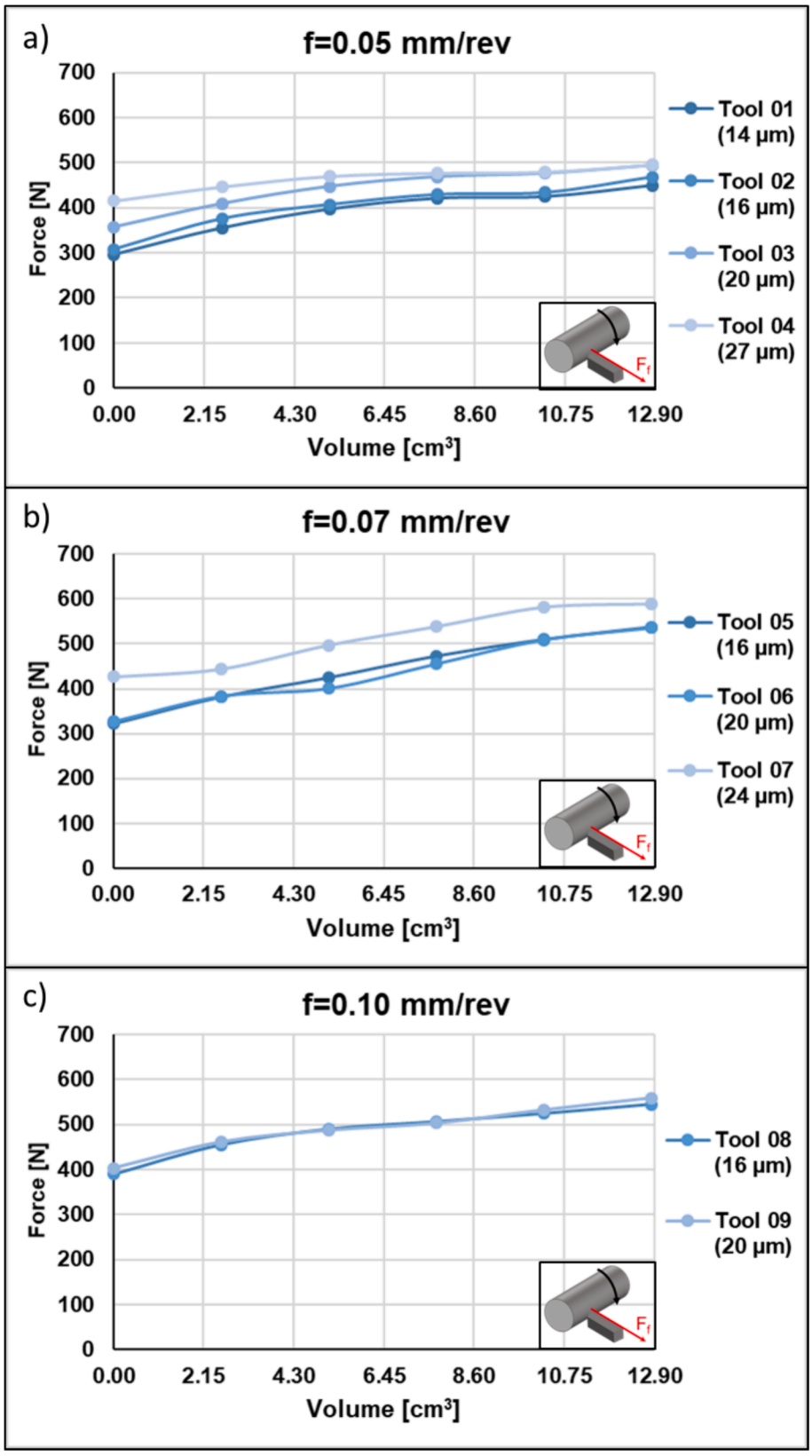

Fig. 12. Feed force (F_f) for all tested tools with a feed of 0.05 mm/rev (a), 0.07 mm/rev (b), and 0.10 mm/rev (c).

cutting force. In the tangential component, the proposed model has offered an average relative error for all the tools of 1.5 % against 1.7 % for the traditional model. In addition, for the feed force, the proposed one offered a 4.8 % error while the traditional one amounted to 6.8 %. Nonetheless, it should be noticed that in some cases (one case for the proposed model and four for the traditional one) in both models for the feed force, the relative error was greater than 15 %. Therefore, the proposed model offers better predictions for both the tangential

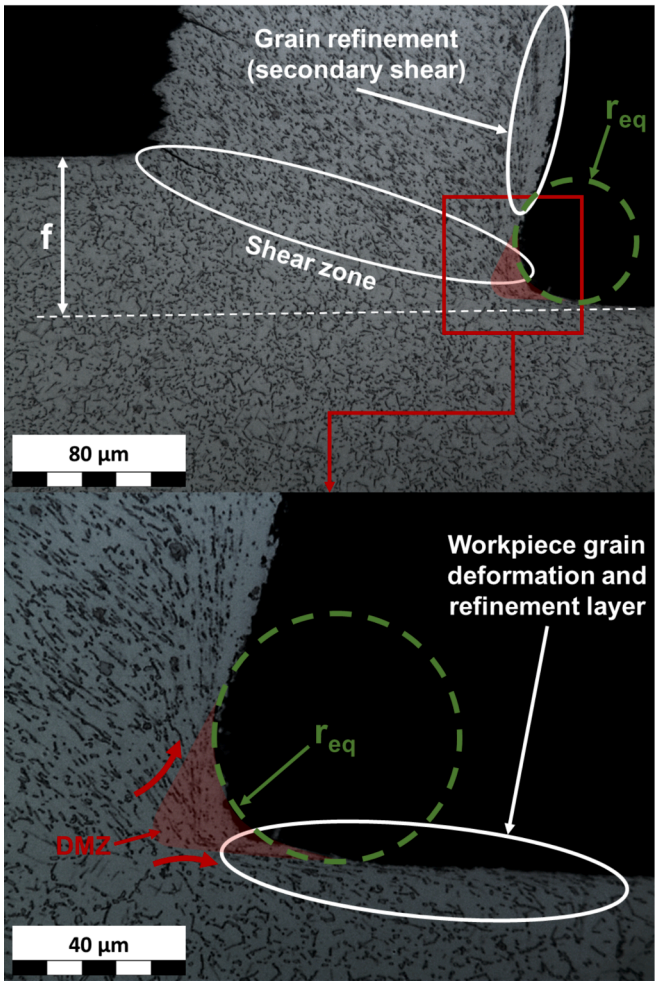

Fig. 13. DMZ during the cutting of Inconel® 718 slots.

component and the feed component of the cutting force.

7. Conclusions

In the present work, the influence of cutting edge preparation on the orthogonal machining of grooves in Inconel® 718 superalloy at high speed with whiskers reinforced alumina tools has been analysed. To this end, the profiles of nine inserts were measured to determine the dimensions of the cutting edge finish and then tests were carried out in which five grooves were made with each tool. During the tests, the wear after each groove and the generated cutting forces were measured and chips were collected for analysis. Moreover, a predictive mechanistic cutting forces model has been proposed and compared with a traditional one. The main conclusions obtained from the research carried out are listed below:

- After machining five slots with all nine tools, none of them reached the flank wear limit of 0.12 mm set as the end of the tool's life.

Table 5
Data of the tests used for obtaining the model coefficients.

Tool	f [mm/rev]	r_{eq} [µm]	a_p [mm]	VB [mm]	F_{cr} [N]	F_{fr} [N]
01	0.05	14	3.18	0.000	502.9	295.6
				0.040	556.8	396.7
				0.049	565.2	424.6
04	0.05	27	3.18	0.000	526.8	415.2
				0.042	566.9	470.1
				0.047	571.1	479.6
09	0.10	20	3.18	0.000	802.9	402.5
				0.046	872.3	486.8
				0.056	892.0	532.3

Table 6
Coefficients for the mechanistic cutting force model.

F_{ct}			F_{ft}		
k_{sct} [N/mm]	k_{fct} [N]	k_{wct} [N/mm]	k_{sft} [N/mm]	k_{fft} [N]	k_{wft} [N/mm]
6028.3	208.3	1303.4	1014.4	302.1	2060.9

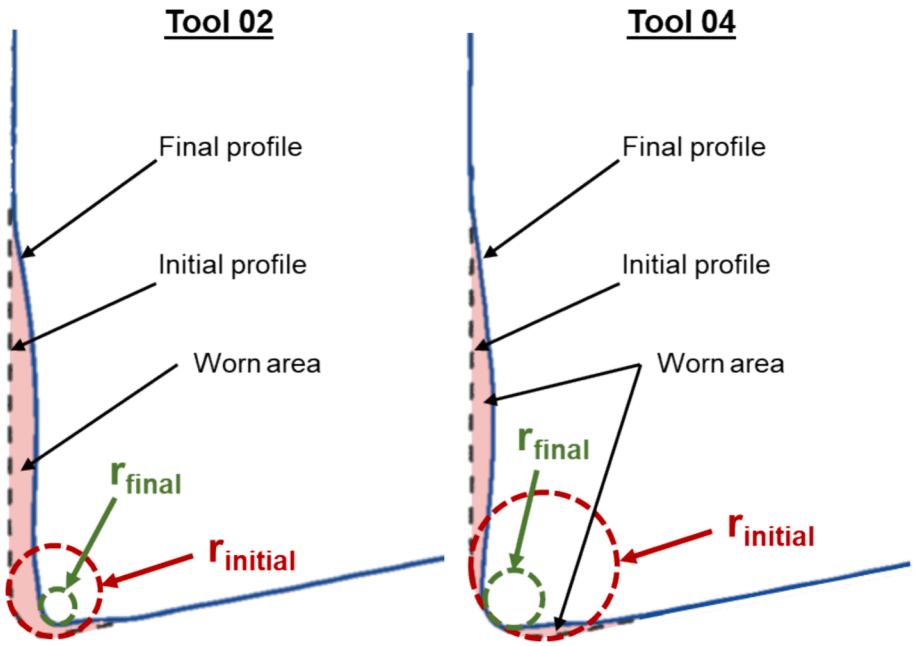

Fig. 14. Initial and final tool profile for tool 02 and tool 04.

Table 7
Coefficients for the proposed cutting force model.

F_{cm}				F_{fm}			
k_{scm1} [N/mm]	k_{scm2} [N/mm]	k_{fcm} [N]	k_{wcm} [N/mm]	k_{sfm1} [N/mm]	k_{sfm2} [N/mm]	k_{ffm} [N]	k_{wfm} [N/mm]
9782.3	1770.9	50.6	1302.9	4458.0	1055.4	317.0	2057.8

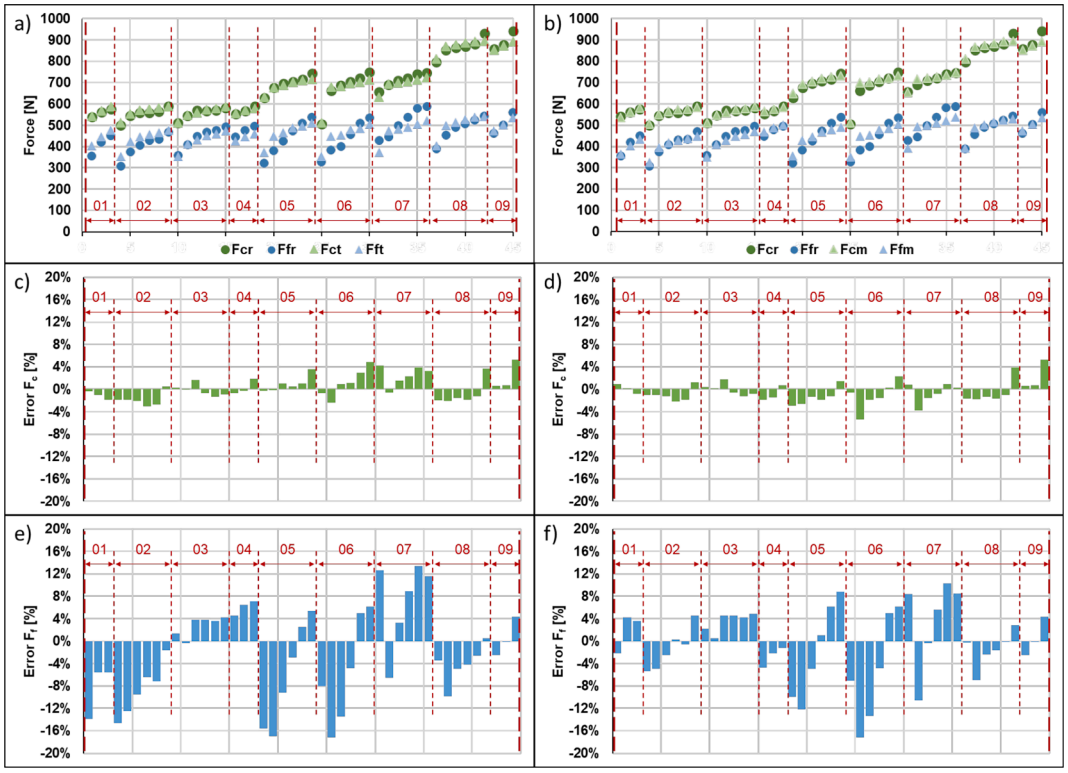

Fig. 15. Models validation: real forces and commonly used predictions (a); real forces and proposed model (b); tangential force errors for commonly (c) and proposed (d) models; feed force errors for commonly (e) and proposed (f) models.

Greater feeds and smaller radii increase the tool's flank wear. However, chip evacuated volume is more important to flank wear.

- All analysed chip shapes were tubular and long except one that was tubular and snarled. The most characteristic feature of the chip was the absence of dragged material which has led to the conclusion that the chip did not blunt and, thus, they slid along the rake face of the tool without sticking.
- When looking at the behaviour of the cutting force component, it has been observed that the equivalent radii of the cutting edge have hardly any influence on it. The thickness of the uncut chip was the main variable that contributed to changes to this component, as there was no variation in the width of the grooves and, therefore, no variation in the depth of cut. Flank wear also influenced the behaviour of this component, but its effect was not critical.
- The feed component was strongly influenced by both flank wear and the equivalent cutting edge radius of the profile, especially at low feeds. In fact, variations of more than 30 % have been observed when varying the cutting edge radii from 14 to 27 μm at a feed of 0.05 mm/rev. At higher feeds, the effect of the equivalent cutting edge radius is diluted. Moreover, the increase in wear has caused the differences in the first groove when using different equivalent radii to become narrower.
- The proposed cutting force model offered an average relative error of 1.5 % and 4.8 % for tangential and feed force respectively, whereas traditional models predictions were higher, 1.7 % and 6.8 %, respectively.

CRediT authorship contribution statement

Pablo Fernández-Lucio: Conceptualization, Data curation, Formal analysis, Investigation, Methodology, Writing – original draft, Writing – review & editing. **Gorka Urbikain:** Supervision, Writing – review & editing. **Soraya Plaza:** Supervision, Writing – review & editing. **Octavio Pereira:** Project administration, Resources, Supervision, Validation, Writing – review & editing.

Declaration of competing interest

The authors declare that they have no known competing financial interests or personal relationships that could have appeared to influence the work reported in this paper.

Acknowledgements

Authors are grateful to the Basque government group IT IT1337-19, to project CPP2021-008932 funded by the Spanish Ministry of Science MCIN/AEI/10.13039/501100011033 and European Union "NextGenerationEU"/PRTR, and the UPV/EHU itself for the financial aid for the pre-doctoral grant PIF 19/96.

References

[1] A. Tayal, N.S. Kalsi, M.K. Gupta, Machining of superalloys: A review on machining parameters, cutting tools, and cooling methods, Mater. Today: Proc. (2020), https://doi.org/10.1016/J.MATPR.2020.10.815.

[2] E.O. Ezugwu, Key improvements in the machining of difficult-to-cut aerospace superalloys, Int. J. Mach. Tool Manu 45 (2005) 1353–1367, https://doi.org/10.1016/j.ijmachtools.2005.02.003.

[3] D. Ulutan, T. Ozel, Machining induced surface integrity in titanium and nickel alloys: a review, Int. J. Mach. Tool Manu 51 (2011) 250–280, https://doi.org/10.1016/j.ijmachtools.2010.11.003.

[4] I. Del Sol, A. Rivero, L.N.L. de Lacalle, A.J. Gamez, Thin-wall machining of light alloys: a review of models and industrial approaches, Materials 2019, Vol. 12, Page 2012 12 (2019) 2012. https://doi.org/10.3390/MA12122012.

[5] A. Rizzo, S. Goel, M.L. Grilli, R. Iglesias, L. Jaworska, V. Lapkovskis, P. Novak, B. O. Postolnyi, D. Valerini, The critical raw materials in cutting tools for machining applications: a review, Materials 13 (2020), https://doi.org/10.3390/ma13061377.

[6] A. Renz, I. Khader, A. Kailer, Tribochemical wear of cutting-tool ceramics in sliding contact against a nickel-base alloy, J. Eur. Ceram. Soc. 36 (2016) 705–717, https://doi.org/10.1016/j.jeurceramsoc.2015.10.032.

[7] K. Sørby, Z. Vagnorius, High-pressure cooling in turning of inconel 625 with ceramic cutting tools, Procedia CIRP 77 (2018) 74–77, https://doi.org/10.1016/j.procir.2018.08.221.

[8] C. Sateesh Kumar, S. Kumar Patel, Hard machining performance of PVD AlCrN coated Al2O3/TiCN ceramic inserts as a function of thin film thickness, Ceram. Int. 43 (2017) 13314–13329, https://doi.org/10.1016/J.CERAMINT.2017.07.030.

[9] Y.M. Ko, W.T. Kwon, Y.W. Kim, Development of Al2O3–SiC composite tool for machining application, Ceram. Int. 30 (2004) 2081–2086, https://doi.org/10.1016/J.CERAMINT.2003.11.011.

[10] A. Fernández-Valdivielso, L.N. López de Lacalle, P. Fernández-Lucio, H. González, Turning of austempered ductile iron with ceramic tools, Proc. Inst. Mech. Eng. B J. Eng. Manuf. 235 (2021) 484–493, https://doi.org/10.1177/0954405420957154.

[11] K. Zhuang, D. Zhu, X. Zhang, H. Ding, Notch wear prediction model in turning of Inconel 718 with ceramic tools considering the influence of work hardened layer, Wear 313 (2014) 63–74, https://doi.org/10.1016/j.wear.2014.02.007.

[12] M. Agmell, A. Ahadi, O. Gutnichenko, J.-E. Ståhl, O. Gutnichenko, The influence of tool micro-geometry on stress distribution in turning operations of AISI 4140 by FE analysis, Int. J. Adv. Manufacturing Technology 89 (2016) 3109–3122, https://doi.org/10.1007/s00170-016-9296-7.

[13] C. Hu, W. Zhang, K. Zhuang, J. Zhou, H. Ding, On the steady-state workpiece flow mechanism and force prediction considering piled-up effect and dead metal zone formation, J. Manuf. Sci. Eng. Trans. ASME 143 (2021), https://doi.org/10.1115/1.4048952/1089697.

[14] K. Zhuang, C. Fu, J. Weng, C. Hu, Cutting edge microgeometries in metal cutting: a review, The Int. J. Adv. Manuf. Tech. 2021 116:7 116 (2021) 2045–2092. https://doi.org/10.1007/S00170-021-07558-6.

[15] K.D. Bouzakis, N. Michailidis, G. Skordaris, S. Kombogiannis, S. Hadjiyiannis, K. Efstathiou, E. Pavlidou, G. Erkens, S. Rambadt, I. Wirth, Optimisation of the cutting edge roundness and its manufacturing procedures of cemented carbide inserts, to improve their milling performance after a PVD coating deposition, Surf. Coat. Technol. 163–164 (2003) 625–630, https://doi.org/10.1016/S0257-8972(02)00687-4.

[16] T. Zhao, J.M. Zhou, V. Bushlya, J.E. Ståhl, Effect of cutting edge radius on surface roughness and tool wear in hard turning of AISI 52100 steel, Int. J. Adv. Manuf. Technol. 91 (2017) 3611–3618, https://doi.org/10.1007/S00170-017-0065-Z/METRICS.

[17] T. Vopat, R. Straka, M. Kuruc, J. Peterka, The effect of cutting edge radius sizes on tool life in machining nickel alloy Inconel 718, 33rd DAAAM International Symposium on Intelligence Manufacturing and Automation (2022) 180–0187. https://doi.org/10.2507/33rd.daaam.proceedings.025.

[18] B. Hariprasad, S.J. Selvakumar, D.S. Raj, Effect of cutting edge radius on end milling Ti-6Al-4V under minimum quantity cooling lubrication-chip morphology and surface integrity study, Wear (2022), https://doi.org/10.1016/j.wear.2022.204307.

[19] A. Sela, G. Ortizde-Zarate, I. Arrieta, D. Soriano, P. Aristimuño, B. Medina-Clavijo, P.J. Arrazola, A mechanistic model to predict cutting force on orthogonal machining of aluminum 7475–T7351 considering the edge radius, Procedia CIRP (2019), https://doi.org/10.1016/j.procir.2019.04.066.

[20] A. Uysal, E. Altan, A new slip-line field modeling of orthogonal machining with a rounded-edge worn cutting tool, Mach. Sci. Technol. 18 (2014) 386–423, https://doi.org/10.1080/10910344.2014.925375.

[21] T. Jagadesh, G.L. Samuel, Mechanistic and finite element model for prediction of cutting forces during micro-turning of titanium alloy, Mach. Sci. Technol. 19 (2015) 593–629, https://doi.org/10.1080/10910344.2015.1085318.

[22] B. Denkena, J.C. Becker, L. de León-García, Study of the influence of the cutting edge microgeometry on the cutting forces ande wear behavior in turning operations, in: 8th CIRP Int.Workshop on Modeling of Machining Operations, Chemnitz, 2005: pp. 503–507.

[23] L. Wan, D. Wang, Numerical analysis of the formation of the dead metal zone with different tools in orthogonal cutting, Simul. Model. Pract. Theory 56 (2015) 1–15, https://doi.org/10.1016/J.SIMPAT.2015.04.006.

[24] L. Jiang, D. Wang, Finite-element-analysis of the effect of different wiper tool edge geometries during the hard turning of AISI 4340 steel, Simul. Model. Pract. Theory 94 (2019) 250–263, https://doi.org/10.1016/J.SIMPAT.2019.03.006.

[25] ISO Standard 3685:1993, ISO 3685: 1993 - Tool-life testing with single-point turning tools, International Standard (1993).

[26] A. Uysal, E. Altan, Effect of Ploughing Force on Cutting Forces in Micro-cutting with a Rounded-edge Cutting Tool, Mater Today Proc, Elsevier Ltd, in, 2015, pp. 224–229.

[27] C.F. Wyen, K. Wegener, Influence of cutting edge radius on cutting forces in machining titanium, CIRP Ann. 59 (2010) 93–96, https://doi.org/10.1016/J.CIRP.2010.03.056.

[28] P. Li, Z. Chang, Numerical modeling of the effect of cutting-edge radius on cutting force and stress concentration during machining, Micromachines (Basel) 13 (2022) 211, https://doi.org/10.3390/MI13020211.

[29] Y. Liu, D. Xu, M. Agmell, R.M. Saoubi, A. Ahadi, J.E. Stahl, J. Zhou, Numerical and experimental investigation of tool geometry effect on residual stresses in orthogonal machining of Inconel 718, Simul. Model. Pract. Theory 106 (2021) 102187, https://doi.org/10.1016/J.SIMPAT.2020.102187.

[30] E. Budak, Y. Altintaş, E.J.A. Armarego, Prediction of milling force coefficients from orthogonal cutting data, J. Manuf. Sci. Eng. 118 (1996) 216–224, https://doi.org/10.1115/1.2831014.